Compartmentalization of stearoyl-coenzyme A desaturase 1 activity in HepG2 cells

Jennifer K. Yee,*,† Catherine S. Mao,*,† Heidi S. Hummel,§ Shu Lim,† Sharon Sugano,†
Virender K. Rehan,*,† Gary Xiao,*,† and Wai-Nang Paul Lee[1],*,†

Department of Pediatrics,* David Geffen School of Medicine, University of California Los Angeles,
Los Angeles, CA; Los Angeles Biomedical Research Institute,† Harbor-University of California Los Angeles
Medical Center, Torrance, CA; and CompleGen, Inc.,§ Seattle, WA

Abstract Stearoyl-coenzyme A desaturase 1 (SCD1) catalyzes the conversion of stearate (18:0) to oleate (18:1n-9) and of palmitate (16:0) to palmitoleate (16:1), which are key steps in triglyceride synthesis in the fatty acid metabolic network. This study investigated the role of SCD1 in fatty acid metabolism in HepG2 cells using SCD1 inhibitors and stable isotope tracers. HepG2 cells were cultured with [U-^{13}C]stearate, [U-^{13}C]palmitate, or [1,2-^{13}C]acetate and (*1*) DMSO, (*2*) compound CGX0168 or CGX0290, or (*3*) *trans*-10,*cis*-12 conjugated linoleic acid (CLA). ^{13}C incorporation into fatty acids was determined by GC-MS and desaturation indices calculated from the respective ion chromatograms. FAS, SCD1, peroxisome proliferator-activated receptor α, and peroxisome proliferator-activated receptor γ mRNA levels were assessed by semiquantitative RT-PCR. The addition of CGX0168 and CGX0290 decreased the stearate and palmitate desaturation indices in HepG2 cells. CLA led to a decrease in the desaturation of stearate only, but not palmitate. Comparison of desaturation indices based on isotope enrichment ratios differed, depending on the origin of saturated fatty acid. SCD1 gene expression was not affected in any group.▮▮ In conclusion, the differential effects of SCD1 inhibitors and CLA on SCD1 activity combined with the dependence of desaturation indices on the source of saturated fatty acid strongly support the compartmentalization of desaturation systems. The effects of SCD1 inhibition on fatty acid composition in HepG2 cells occurred through changes in the dynamics of the fatty acid metabolic network and not through transcriptional regulatory mechanisms.—Yee, J. K., C. S. Mao, H. S. Hummel, S. Lim, S. Sugano, V. K. Rehan, G. Xiao, and W-N. P. Lee. **Compartmentalization of stearoyl-coenzyme A desaturase 1 activity in HepG2 cells.** *J. Lipid Res.* 2008. **49:** 2124–2134.

The enzyme stearoyl-coenzyme A desaturase (SCD) is important in the conversion of saturated fatty acids to monounsaturated fatty acids (MUFAs). The isoform SCD1 catalyzes the desaturation of palmitate (16:0) to palmitoleate (16:1n-9) and of stearate (18:0) to oleate (18:1n-9). Palmitoleate and oleate are the main MUFAs that constitute membrane phospholipids, triglycerides, wax esters, and cholesteryl esters. Because an inappropriate ratio of MUFA to saturated fatty acid can affect membrane lipid fluidity and lipoprotein metabolism, the effects of SCD have been implicated not only in obesity but also in diabetes, atherosclerosis, and cancer (1–5).

Mouse models of SCD1 deficiency have demonstrated effects on body weight and lipid metabolism. Asebia mice have a naturally occurring homozygous mutation in SCD1 (6). These mice lack sebaceous glands and have alopecia and dry skin. In addition, they are lean and have impaired hepatic ability to synthesize cholesteryl esters and triglycerides (7). Ntambi and colleagues (8) created a knockout mouse for SCD1. These mice have decreased adiposity, increased insulin sensitivity, and are resistant to diet-induced weight gain. These properties of the SCD1$^{-/-}$ mouse have generated much interest in SCD as a potential target for obesity prevention in humans.

In the mouse and rat, inhibition of SCD1 using antisense oligonucleotides has been done in vitro and in vivo. Gutierrez-Juarez et al. (9) showed that administration of SCD1 antisense oligonucleotide to overfed rats with hepatic insulin resistance restored rates of gluconeogenesis and glycogenolysis to those observed in control rats. However, studies of the effects of SCD1 inhibition in human cell culture have been limited. SCD1 inhibitors based on the pyridazine carboxamide structure have been studied in HepG2 cell culture (10). Choi et al. (11) showed some

[1] To whom correspondence should be addressed.
e-mail: lee@labiomed.org

decreased activity in cell cultures of HepG2 cells with the *trans*-10,*cis*-12 isomer of conjugated linoleic acid (CLA).

The desaturation of long-chain fatty acids (LCFAs) is part of the many connected pathways that generate the fatty acid distribution seen in triglycerides and phospholipids. Compartmentalization of fatty acid synthesis pathways, either physical or functional, in intact cells may contribute to the dynamics of fatty acid synthesis, chain elongation, and desaturation. The effects of SCD1 inhibition on these dynamics in fatty acid metabolism are poorly understood. Stable isotopes such as the uniformly labeled fatty acids [U-^{13}C]stearate and [U-^{13}C]palmitate have been used to study LCFA desaturation, chain elongation, and shortening (12, 13). In this study, stable isotopes were used to distinguish between the SCD1 pathways of palmitate-to-palmitoleate and stearate-to-oleate conversion as well as chain elongation and chain shortening. The purpose of this study was to investigate the effects of SCD1 inhibition on the metabolism of LCFA in human hepatoma HepG2 cells using stable isotope-labeling techniques. The efficacies of two new SCD1 inhibitors (CompleGen, Inc.) were compared with the efficacy of *trans*-10,*cis*-12 CLA, which has also been studied for antiadipogenic properties (11, 14). We found that SCD1 inhibition altered the interconversion of LCFA in the fatty acid metabolic network in HepG2 cells with different effects on the SCD1 pathways, indicating compartmentalization.

MATERIALS AND METHODS

SCD1 inhibitors

The SCD1 inhibitors CGX0168 (molecular mass, 238 Da) and CGX0290 (molecular mass, 212 Da) were provided by CompleGen, Inc. These compounds had been identified through XenoGene™ assay, in which yeast dependent on the human SCD1 gene for growth were grown in the presence of compounds. Cell density was monitored after 12–18 h at 32°C. Activity was determined by comparing the growth of cultures containing compounds with a control culture (DMSO at the same concentration as the test cultures). The IC$_{50}$ values for the inhibitors had been determined by biochemical assay (15) and cell assay.[2] The IC$_{50}$ for CGX0168 was 1.72 μM by biochemical assay and 1.87 μM by cell assay. The IC$_{50}$ for CGX0290 was 1.52 μM by biochemical assay and 0.58 μM by cell assay. The inhibitors were in powder form at room temperature. They were dissolved in DMSO to a concentration of 10 μM for addition to the culture medium. Ninety-eight to 99% enriched [U-^{13}C]potassium stearate, [U-^{13}C]sodium palmitate, and [1,2-^{13}C]sodium acetate were purchased from Martek Biosciences (Columbus, OH).

Cell culture experiments

Human hepatoma HepG2 cells (American Type Culture Collection; HB-8065) were grown in 75 ml tissue cell culture

---

[2] The cell assay was performed by incubating HepG2 cells with inhibitor and [^{14}C]palmitate. After saponification, [^{14}C]palmitate, [^{14}C]stearate, and the desaturated species [^{14}C]palmitoleate and [^{14}C]oleate were measured by radioactivity in the respective peaks by HPLC (flow counter). Activity was calculated as the ratio of desaturated to saturated ^{14}C fatty acid. The IC$_{50}$ was the concentration calculated to give 50% of the control value.

flasks in Dulbecco's modified Eagle's medium augmented with 10% fetal bovine serum, 1% penicillin (100 U/ml)/streptomycin (100 μg/ml) plus amphotericin B (0.25 μg/ml), 25 mM HEPES buffer, and 1,000 mg/l glucose at 37°C in a humidified atmosphere with 5% CO$_2$. When the cells were confluent, the medium was removed, and cells were washed with phosphate-buffered saline. Then, the cells were incubated in medium containing 0.1 mM uniformly labeled [U-^{13}C]stearate and 0.5 mM [1,2-^{13}C] sodium acetate (Martek Biosciences). These fatty acids were added to the medium dissolved in alcohol. DMSO was added to flask group A as a control group. Inhibitor CGX0168 (CompleGen, Inc.), inhibitor CGX0290 (CompleGen, Inc.), or *trans*-10,*cis*-12 CLA (Matreya, LLC) was added to the medium at a concentration of 10 μM to flasks labeled B, C, or D, respectively. Each group of flasks consisted of four flasks. The cells were incubated for 72 h. Medium was changed at 0, 24, and 48 h. At 72 h, medium was collected and cells were harvested for analysis. This experiment was repeated with 0.1 mM [U-^{13}C]palmitate instead of [U-^{13}C]stearate.

Lipid extractions

Lipid extractions were performed as previously described by Lowenstein, Brunengraber, and Wadke (16). This technique extracts all fatty acids from the cells, including those from all cellular triglycerides and phospholipids. Three flasks from each experimental group were prepared for analysis. Cell pellets were saponified overnight at 70°C with 100 μl of 30% KOH (by weight) and 100 μl of 200-proof ethanol. The aqueous phase was acidified with HCl, and the fatty acids were extracted with petroleum ether three times. The ether layers were dried under a nitrogen stream before methylation with 0.5 N HCl in methanol (Supelco, Bellefonte, PA) for GC-MS analysis.

GC-MS analysis

GC-MS analysis was carried out using a Hewlett-Packard model 5973 selective mass detector connected to a model 6890 gas chromatograph. Fatty acids were analyzed as their methyl esters after derivatization. Palmitate, palmitoleate, stearate, oleate, and vaccenate were separated on the gas chromatograph with a Bpx70 column (30-m length, 250-μm diameter, 0.25-μm film thickness) from SGE, Inc. (Austin, TX). The GC conditions were as follows: helium flow rate, 1 ml/min; initial oven temperature, 150°C, which was programmed to increase at 3°C/min to a final temperature of 221°C. The expected retention times for palmitate, palmitoleate, stearate, oleate, and vaccenate under these conditions were as follows: 6.2, 6.7, 8.9, 9.5, and 9.7 min, respectively. Mass spectra of fatty acids were acquired using electron impact ionization and selective ion monitoring. Ion clusters monitored for the quantitation of isotopomers of palmitate were *m/z* 269–276 and 286–290 with m+0 at *m/z* 270 and m+16 at *m/z* 286. The clusters corresponding to palmitoleate were *m/z* 236–240 and 251–255. The clusters corresponding to stearate were *m/z* 298–302 with m+0 at *m/z* 298 and *m/z* 312–316 with m+18 at *m/z* 316. For oleate and vaccenate, the clusters were *m/z* 264–267 and 282–285, with m+18 at m/z 296.

Isolation and analysis of RNA

Analysis of mRNA was done on the cell cultures incubated with isotopes [U-^{13}C]palmitate and [1,2-^{13}C]sodium acetate. One flask from each experimental group was used. Total RNA was extracted directly from the cells in the flasks using TRIzol reagent (Invitrogen Life Technologies, Carlsbad, CA). cDNA was made by reverse transcriptase SuperScript III (Invitrogen Life Technologies) with random primers (Promega, Madison, WI) using 2 μg per assay of total RNA. PCR was carried out using the following gene-

specific primers: 18S, 5′-TTAAGCCATGCATGTCTAAGTAC-3′ and 5′-TGTTATTTTTCGTCACTACCTCC-3′ (17); hSCD1, 5′-GC-AGGACGATATCTCTAGCT-3′ and 5′-GTCTCCAACTTATC-TCCTCCATTC-3′ (5); FAS, 5′-CGGTACGCGACGGCTGCCTG-3′ and 5′-GCTGCTCCACGAACTCAAACACCG-3′ (18); peroxisome proliferator-activated receptor γ (PPARγ), 5′-CCCTCATGGCAAT-TGAATGTCGTG-3′ and 5′-TCGCAGGCTCTTTAGAAACTCCCT-3′ (17); and PPARα, 5′-GGAAAGCCCACTCTGCCCCCT-3′ and 5′-AGTCACCGAGGAGGGGCTCGA-3′ (19).

The PCRs were cycled in a Robocyler Gradient 96 machine (Stratagene, La Jolla, CA) for 2 min at 95°C, followed by 30 cycles of 95°C for 30 s, 58°C for 45 s, 72°C for 1 min, and 72°C for 10 min. PCR products were separated on a 1.5% agarose gel stained with ethidium bromide and visualized under ultraviolet light. The PCRs were done in triplicate on the same cDNA. The PCR product sizes were as follows: 18S, 489 bp; FAS, 231 bp; hSCD1, 90 bp; PPARα, 235 bp; and PPARγ, 757 bp. Band densities were quantified using the Eagle Eye II program (Stratagene). 18S served as the internal loading control, and gene expression was normalized to 18S levels.

Desaturation index

The desaturation index is the ratio of monounsaturated fatty acid to saturated fatty acid determined by the integrated areas under the gas chromatogram peaks. The ratios of palmitoleate-palmitate (16:1/16:0), oleate-stearate (18:1 n-9/18:0), and vaccenate-stearate (18:1 n-7/18:0) were determined for this study in every experimental group.

Spectral data analysis

Distribution of the mass isotopomer was determined from the spectral data using a method previously described by Lee et al. (20) that corrects for the contribution of derivatizing agent and ^{13}C natural abundance to the mass isotopomer distribution of the compound of interest. Each compound of interest includes the sum of isotopomer peaks within a cluster. The resulting mass isotopomer distribution was expressed in molar fractions (m_0, m_1, m_2, m_3, etc.) corresponding to the fraction of molecules that contain 0, 1, 2, 3, ...^{13}C substitutions.

The design of the study using [1,2-^{13}C]acetate and [U-^{13}C]stearate or [U-^{13}C]palmitate allowed the separation of three separate pools for each fatty acid. The added (exogenous) fatty acid pool was represented by the U-^{13}C-labeled fatty acid (M+18 or M+16), the newly synthesized fatty acid pool was represented by the fatty acid with mass shift of M+2 and M+4, and fatty acids made from the preexisting fatty acid pool were represented by the "unlabeled" (M+0) fatty acid (**Fig. 1**).

Determination of the desaturation index based on isotopomer enrichment

The peaks in the fatty acid mass spectra were first normalized in order to express the enrichment data as molar fractions of
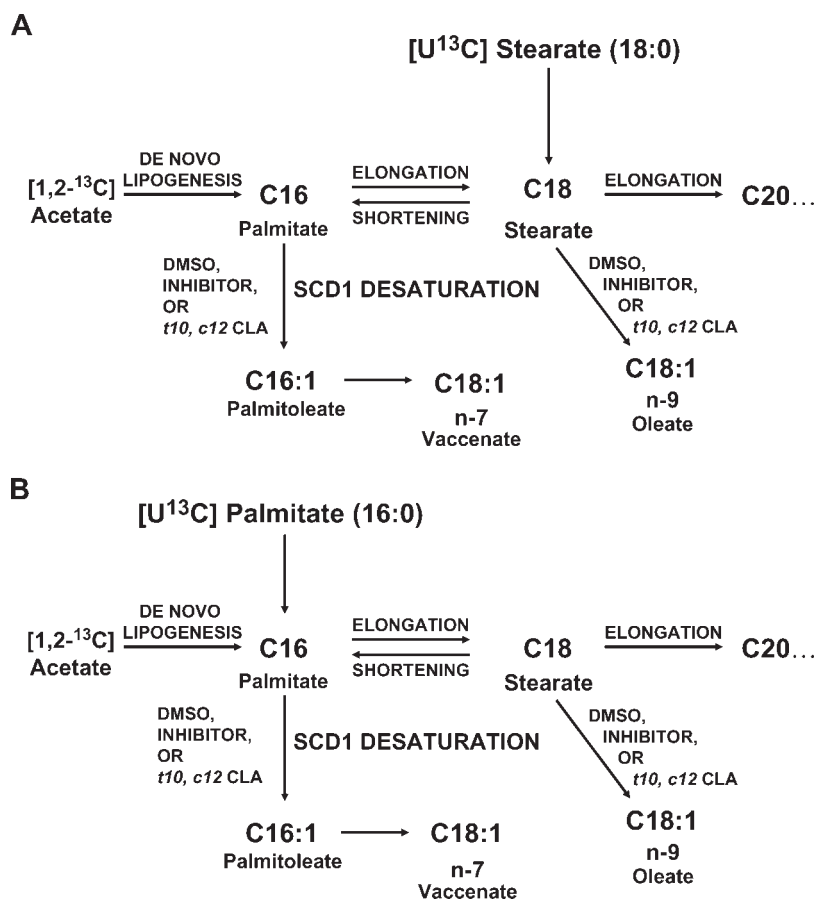

Fig. 1. Pathways of SCD1 desaturation. Oleate is made from the desaturation of stearate. Palmitoleate is made from the desaturation of palmitate. Vaccenate is only made by chain elongation of palmitoleate and cannot be made directly from stearate. A: Addition of labeled stearate and labeled acetate allows distinction between the pathways by GC-MS analysis and provides information on chain shortening. B: Alternatively, addition of labeled acetate and labeled palmitate provides information on de novo lipogenesis and chain elongation.

each particular compound. In experiments with [U-^{13}C]stearate, M+16 palmitate was formed by chain shortening. The conversion of palmitate to palmitoleate and of stearate to oleate by desaturation resulted in the formation of M+16 palmitoleate and M+18 oleate. M+16 vaccenate was produced by chain elongation of palmitoleate. In experiments with [U-^{13}C]palmitate, M+16 palmitoleate was formed by desaturation, and M+16 oleate was formed by desaturation of M+16 stearate produced by chain elongation. The contribution of labeled palmitate to palmitoleate by SCD1 desaturation was estimated from the ratio of molar enrichment of (M+16 palmitoleate) to (M+16 palmitate). In experiments with [U-^{13}C]palmitate, the contribution of labeled stearate to oleate by SCD1 desaturation was estimated from (M+16 oleate)/(M+16 stearate); in experiments with [U-^{13}C]stearate, this was estimated from (M+18 oleate)/(M+18 stearate). Interconversion of palmitate and stearate by chain elongation and shortening was studied similarly. The product-precursor ratio of $(m_{18} + m_{16})$ stearate/$(m_{16}$ palmitate) in [U-^{13}C]palmitate experiments was calculated to represent chain elongation. The ratio of (M+16 palmitate)/(M+18) stearate in [U-^{13}C]stearate experiments was calculated to represent chain shortening.

Determination of precursor enrichment and de novo lipogenesis

Precursor acetyl-CoA enrichment was calculated from the consecutive mass isotopomer ratio M+4/M+2 of palmitate. M+2 and M+4 isotopomers result from [1,2-^{13}C]acetate incorporation into palmitate in de novo lipogenesis. Fraction of new synthesis can be determined after the precursor enrichment is determined (21, 22). [1,2-^{13}C]acetate can also be produced when [U-^{13}C]stearate or [U-^{13}C]palmitate is oxidized from β-oxidation of stearate and palmitate. The [1,2-^{13}C]acetyl-CoA produced part of the precursor acetyl-CoA pool. Therefore, changes in precursor enrichment may be observed if SCD1 inhibition affects the β-oxidation of fatty acids.

RESULTS

Desaturation indices

The fatty acids from the cell extracts were analyzed as their methyl esters. Gas chromatography revealed peaks for palmitate, palmitoleate, stearate, oleate, and vaccenate (**Fig. 2**). Desaturation indices for both the set of flasks with [U-^{13}C]stearate and the set of flasks with [U-^{13}C]palmitate are shown in **Figs. 3** and **4**. Desaturation indices for oleate/stearate, palmitoleate/palmitate, and vaccenate/stearate were calculated from the areas under the fatty acid peaks corresponding to stearate, oleate, palmitate, palmitoleate, and vaccenate.

There was a significant decrease in the desaturation index for oleate/stearate in the SCD1 inhibitor and CLA groups compared with the control in the experiment with labeled stearate (Fig. 3A). In the labeled palmitate experiment, there was a trend of decreasing oleate/stearate desaturation indices in experimental groups, but the differences were not statistically significant (Fig. 3B). The desaturation indices of palmitoleate/palmitate from the experiments with labeled stearate (Fig. 3C) and labeled palmitate (Fig. 3D) are also shown. The palmitoleate/palmitate desaturation indices in the SCD1 inhibitor groups were significantly decreased in comparison with that of the control group in both experiments. However, the palmitoleate/palmitate desaturation index for the CLA group was increased or not changed in comparison with the control. Therefore, addition of the inhibitors, but not CLA, led to decrease in the palmitoleate/palmitate desaturation index.

Figures 4C and 4D show the increase in the stearate-palmitate ratio when cells were treated with SCD1 inhibi-
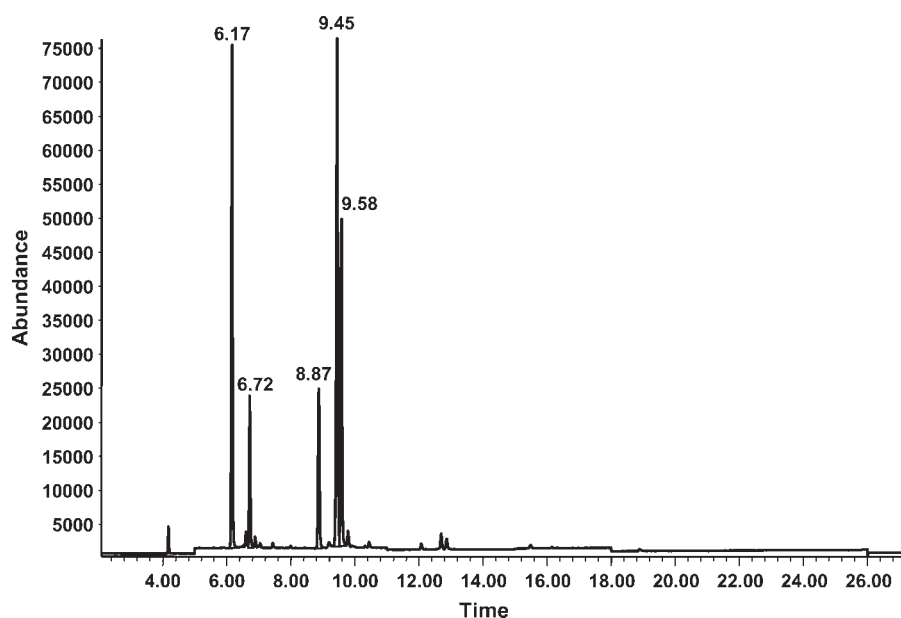

Fig. 2. Ion chromatogram of fatty acids, with retention times on the *x* axis and relative abundance on the *y* axis. Retention times for palmitate, palmitoleate, stearate, oleate, and vaccenate were 6.17, 6.72, 8.8, 9.45, and 9.58 min, respectively.
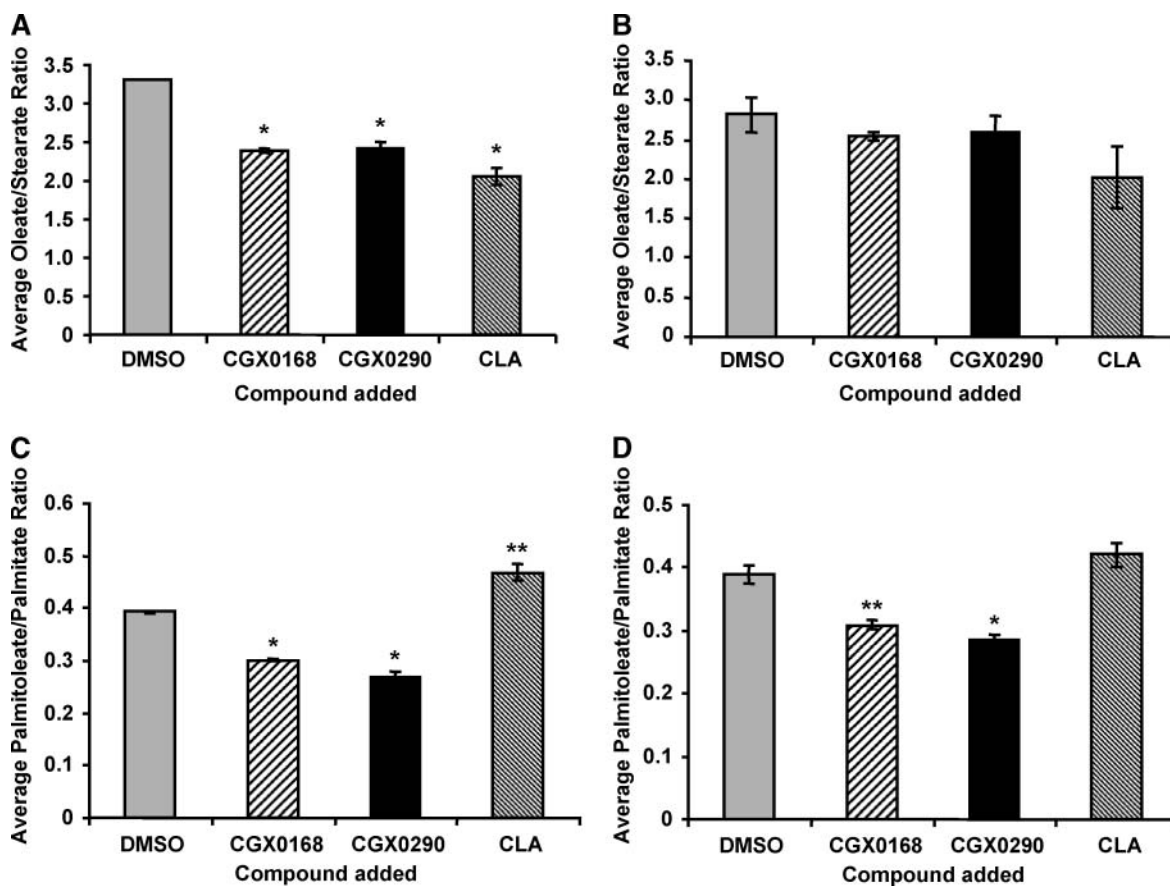
Fig. 3. Desaturation indices of oleate-stearate (18:1 n-9/18:0) and palmitoleate-palmitate (16:1/16:0) in [U-^{13}C]stearate (A, C) and [U-^{13}C] palmitate (B, D) experiments. Each bar represents the average and SEM of triplicate cell culture experiments. * $P \leq 0.001$, ** $P \leq 0.003$. In the experiment with [U-^{13}C]stearate, the average oleate-stearate ratio was significantly decreased ($P < 0.001$). In the experiment with [U-^{13}C]palmitate, the average oleate-stearate ratio was mildly decreased, but not significantly in the CGX0168 ($P = 0.14$) and CGX290 groups ($P = 0.25$); it approached significance in the CLA group ($P = 0.08$). Both experiments showed a significant decrease in the palmitoleate/palmitate desaturation indices with the inhibitors. With [U-^{13}C]stearate, the average palmitoleate-palmitate ratio was significantly decreased in the CGX0168 and CGX0290 groups ($P < 0.001$), but it was increased in the CLA group ($P = 0.0029$). With [U-^{13}C]palmitate, the average ratio was significantly decreased for both the CGX0168 group ($P = 0.003$) and the CGX0290 group ($P < 0.001$). However, in the CLA group, the difference was not significant, with a trend toward an increased ratio ($P = 0.13$).

tors or CLA. Addition of SCD1 inhibitors and CLA led to significant increases in the concentration of stearate, which was likely a significant contributing factor in the decrease of the desaturation index.

The 18 carbon monounsaturated fatty acid vaccenate is produced from chain elongation of palmitoleate and not directly from desaturation of stearate (Fig. 1). The average desaturation index of vaccenate/stearate from each experimental group with inhibitor or CLA was significantly reduced in comparison with the control.

Fatty acid enrichment ratios

The molar enrichment of the precursors and their respective products is shown in **Table 1**. Addition of [U-^{13}C]palmitate or [U-^{13}C]stearate allowed study of the interconversion and desaturation of palmitate and stearate. Mass spectral data yielded two clusters of peaks for each fatty acid spectrum. The "light" cluster represented pre-existing unlabeled and newly synthesized molecules. The "heavy" cluster represented fatty acids made from uni-

formly labeled precursors. Cells enriched with labeled palmitate had M+16 peaks in the spectra of palmitoleate, stearate, oleate, and vaccenate, representing molecules made from labeled palmitate, while cells enriched with labeled stearate had M+18 peaks in oleate, representing molecules made from labeled stearate (**Fig. 5**).

In Table 1, chain elongation of M+16 palmitate resulted in M+16 stearate, whereas chain shortening of M+18 stearate resulted in M+16 palmitate. The desaturation indices for the conversion of M+16 stearate and M+16 palmitate to M+16 oleate and M+16 palmitoleate, respectively, are also shown. The ratio of enrichment of the monounsaturated fatty acid to the enrichment of the corresponding saturated fatty acid is the fraction of monounsaturated fatty acid that is derived from the labeled precursor pool. It is a function of desaturase activity on the labeled tracer molecules as well as turnover of the monounsaturated pool. Thus, in the labeled stearate experiment, desaturation of labeled stearate contributed to 47.9% of the oleate pool (Table 1, stearate experiment, control group A),
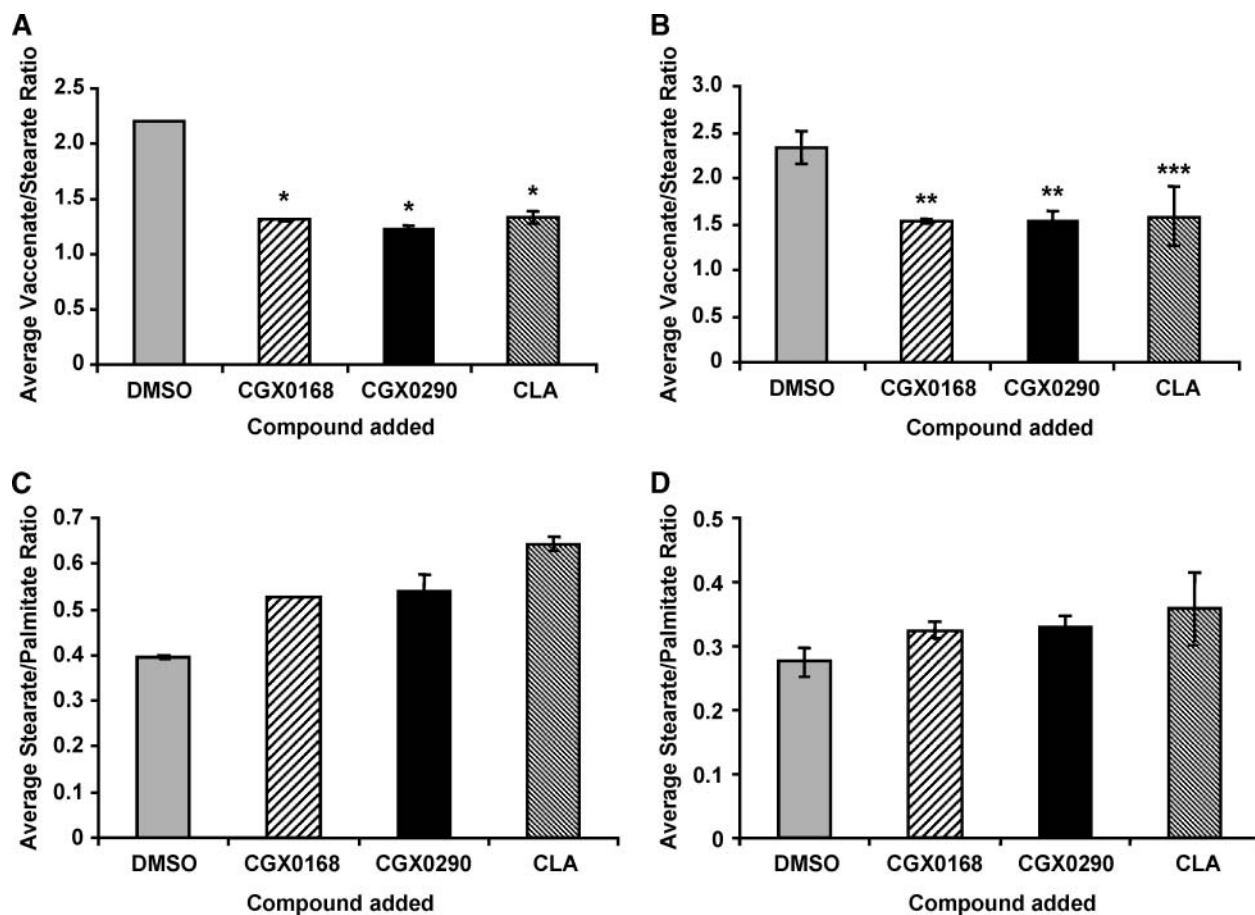
Fig. 4. Desaturation index for vaccenate-stearate (18:1 n-7/18:0) and the ratio of stearate to palmitate (18:0/16:0) in [U-^{13}C]stearate (A, C) and [U-^{13}C]palmitate (B, D) experiments. Each bar represents the average and SEM of the ratio for triplicate cell culture experiments. * $P < 0.001$, ** $P < 0.01$, *** $P = 0.053$. The average ratio of vaccenate to stearate with [U-^{13}C]stearate was significantly decreased with CGX0168 ($P < 0.001$), CGX290 ($P < 0.001$), and CLA ($P < 0.001$). In the experiment using [U-^{13}C]palmitate, there was also a significant decrease with CGX0168 ($P = 0.005$) and GCX0290 ($P = 0.009$). With CLA, the decrease approached significance with $P = 0.053$. Both experiments showed similar stearate-palmitate ratios in each of the four groups.

while desaturation of labeled palmitate contributed to 80.7% of the palmitoleate pool in the labeled palmitate experiment (Table 1, palmitate experiment, control group A). The effects of SCD1 inhibitors and CLA on the conversion of saturated to monounsaturated fatty acids were demonstrated by the decrease in enrichment ratios in Table 1, except for the M+16 oleate/M+16 stearate ratio in the experiment with labeled palmitate.

The conversion of saturated to monounsaturated fatty acid was found to be different between the [U-^{13}C]stearate and [U-^{13}C]palmitate experiments depending on the source of saturated fatty acid in the groups, even when no inhibitor or CLA was added. For example, when the labeled palmitate was derived from chain shortening, the desaturation index (M+16 palmitoleate/M+16 palmitate) was lower (0.202; Table 1, stearate experiment, control group A) than when the labeled palmitate was supplied exogenously (0.807; Table 1, palmitate experiment, control group A). A similar difference was also observed in the conversion of stearate to oleate. The ratio M+16 oleate/M+16 stearate was higher when the label was derived from chain elongation (0.614; Table 1, palmitate experiment, control group A) than the ratio M+18 oleate/ M+18 stearate when the label was supplied exogenously (0.479; Table 1, stearate experiment, control group A).

Under certain conditions, such as when the pool size of the product is large or its turnover slow, the desaturation index as determined by the monounsaturated-to-saturated fatty acid ratio should correlate with the desaturation index estimated from the enrichment ratio of the monounsaturated to saturated fatty acids. To examine the correlation of the desaturation index, we plotted the desaturation indices against the enrichment ratios as shown in **Fig. 6**. The desaturation index increased linearly with the enrichment ratio in this particular instance. The correlation was poor or absent when the U-^{13}C-labeled fatty acid added was not the direct precursor of the monounsaturated fatty acid, for example, in the conversion of stearate to oleate in the [U-^{13}C]palmitate experiment (data not shown).

Chain elongation and chain shortening

Table 2 shows the assessment of chain elongation of palmitate to stearate and chain shortening of stearate to palmitate (Fig. 1) using the labeled fatty acids (Table 2).

TABLE 1. Desaturation of [U-^{13}C]stearate and [U-^{13}C]palmitate to their corresponding MUFAs

[U-^{13}C]Stearate Experiment

| | Fractional Enrichment of M+18 Stearate and M+18 Oleate | | | | | Desaturation Index | | | | |
| | M+18 Stearate Enrichment | | M+18 Oleate Enrichment | | | M+16 Palmitoleate/M+16 Palmitate | | M+18 Oleate/M+18 Stearate | |
Group	Average ± SD	P	Average ± SD	P		Average ± SD	P	Average ± SD	P
A (control)	0.350 ± 0.0056		0.168 ± 0.008			0.202 ± 0.021		0.479 ± 0.015	
B	0.354 ± 0.006	0.199	0.140 ± 0.003	0.002		0.075 ± 0.007	0.0007	0.395 ± 0.006	0.0004
C	0.351 ± 0.006	0.392	0.132 ± 0.006	0.002		0.055 ± 0.007	0.0002	0.377 ± 0.01	0.0003
D	0.424 ± 0.008	0.0001	0.132 ± 0.003	0.001		0.143 ± 0.021	0.0136	0.314 ± 0.013	0.001

[U-^{13}C]Palmitate Experiment

| | Fractional Enrichment of M+16 Palmitate and M+16 Palmitoleate | | | | | Desaturation Index | | | | |
| | M+16 Palmitate Enrichment | | M+16 Palmitoleate Enrichment | | | M+16 Palmitoleate/M+16 Palmitate | | M+16 Oleate/M+16 Stearate | |
Group	Average ± SD	P	Average ± SD	P		Average ± SD	P	Average ± SD	P
A (control)	0.197 ± 0.010		0.159 ± 0.005			0.807 ± 0.040		0.614 ± 0.105	
B	0.199 ± 0.010	0.418	0.129 ± 0.013	0.009		0.646 ± 0.037	0.010	0.586 ± 0.044	0.346
C	0.199 ± 0.007	0.429	0.126 ± 0.006	0.001		0.633 ± 0.029	0.001	0.564 ± 0.046	0.248
D	0.204 ± 0.006	0.181	0.139 ± 0.003	0.001		0.683 ± 0.007	0.002	0.673 ± 0.197	0.336

HepG2 cells were cultured in the presence of either [U-^{13}C]stearate or [U-^{13}C]palmitate. DMSO was added to control group A, inhibitor CGX0168 to group B, CGX0290 to group C, and CLA to group D. The enriched fractions of stearate and oleate and of palmitate and palmitoleate are presented. The action of SCD1 converts M+18 stearate to M+18 oleate, M+16 stearate to M+16 oleate, and M+16 palmitate to M+16 palmitoleate. The desaturation indices calculated from the enriched fatty acid conversions are presented as well. Differences in the desaturation indices were observed, depending on whether the labeled precursor was exogenous versus derived from chain elongation/shortening. Enrichment ratios are decreased, except for the M+16 oleate/M+16 stearate ratio in the experiment with [U-^{13}C]palmitate.

The ratio of (m$_{18}$+m$_{16}$) stearate/m$_{16}$ palmitate represents the contribution of chain elongation to the stearate pool. (M+18 stearate is the result of chain elongation of M+16 palmitate with M+2 acetyl-CoA.) Chain shortening is represented by m$_{16}$ palmitate/m$_{18}$ stearate. SCD1 inhibitor treatment resulted in an increase in (m$_{18}$+m$_{16}$) stearate/m$_{16}$ palmitate (chain elongation), since more palmitate was available for chain elongation reactions. However, such an increase was not observed with CLA whether [U-^{13}C]palmitate or [U-^{13}C]stearate was added, and the contribution of palmitate to chain elongation was unchanged. Addition of either SCD1 inhibitor or CLA led to increased chain shortening.

De novo lipogenesis

Precursor acetyl-CoA enrichment was calculated from the consecutive mass isotopomer ratio M+4/M+2 of palmitate and the fraction of new synthesis calculated using mass isotopomer distribution analysis (MIDA) (21, 22) (**Table 3**). These calculations used information from the "light" fraction of molecules with peaks corresponding to m$_2$, m$_4$, and m$_6$ molecules from incorporation of [1,2-^{13}C] acetyl-CoA in de novo synthesis of palmitate. The contribution of de novo palmitate synthesis ranged from 51.3% to 53.8% (Table 3, stearate experiment) in the experiments with [U-^{13}C]stearate and 45.9% to 49.6% (Table 3, palmitate experiment) in the experiments with [U-^{13}C]palmitate. The corresponding precursor enrichment, labeled acetate as a fraction of total acetate, was found to range from 0.128 to 0.135 in the experiments with [U-^{13}C]stearate (Table 3, stearate experiment). A higher range of 0.174 to 0.198 was found in the experiments with [U-^{13}C]palmitate (Table 3, palmitate experiment).

Gene expression

There were no changes observed in mRNA levels as assessed by semiquantitative RT-PCR (**Fig. 7**). Therefore, the inhibitors and CLA appear not to inhibit gene expression; rather, they inhibit by another mechanism.

DISCUSSION

SCD1 converts stearate to oleate and palmitate to palmitoleate prior to triglyceride synthesis

The inhibition of desaturase activity may have major effects on the intracellular concentration of saturated LCFAs and MUFAs that are required for the assembly of triglycerides. How SCD1 inhibition affects the other fatty acid metabolic pathways, and whether these reactions are compartmentalized, have not been well studied. SCD1 activity is commonly assayed in cell lysate using radioisotope tracers under standard conditions. The conventional desaturation index as determined by fatty acid concentration ratios is commonly used as a surrogate measure of desaturase activity in vivo. It is a static indicator of desaturase activity reflecting simultaneous changes in the concentrations of these fatty acids. It reflects conversion to the monounsaturated product and the rate of disappearance of this product, but it may not accurately reflect the in vivo desaturase activity or the activity in the whole cell.
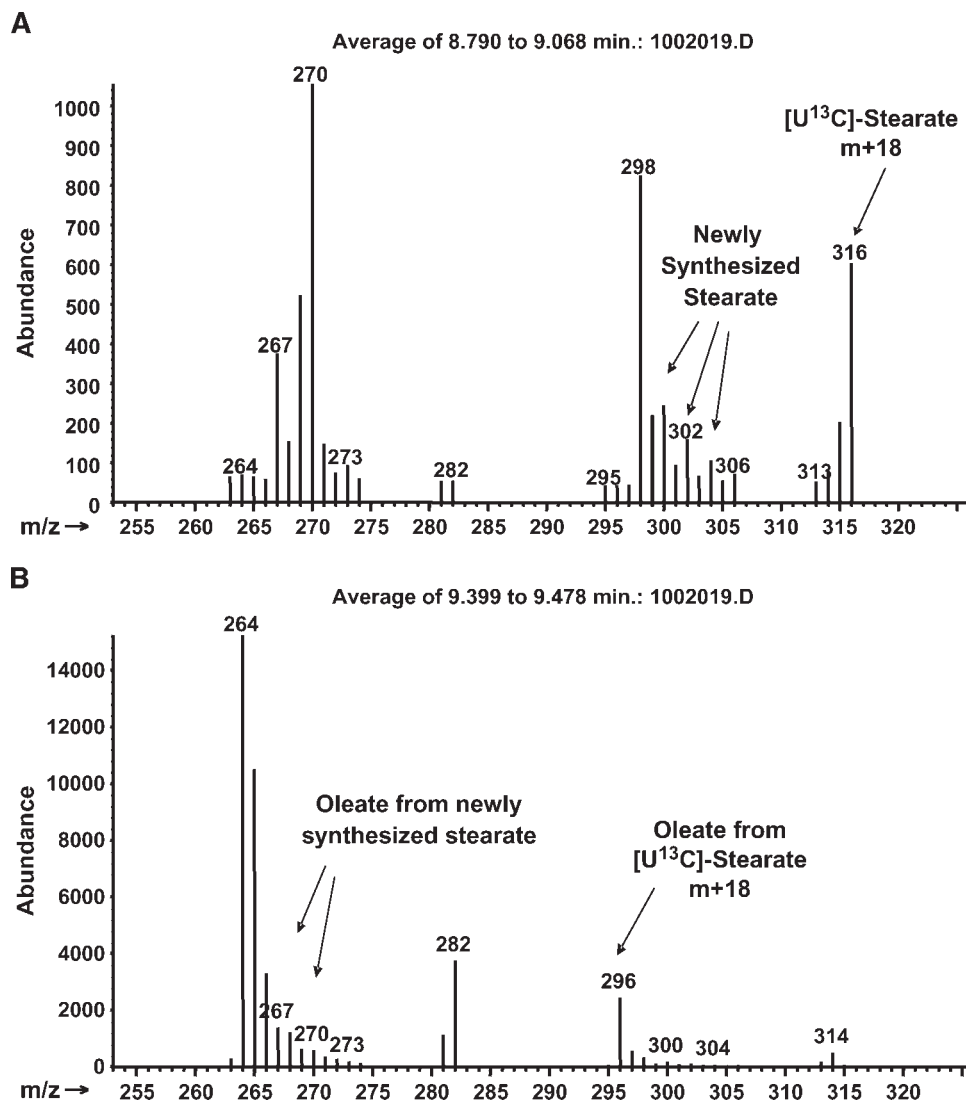
Fig. 5. Mass spectra of stearate and oleate showing uptake of M+18 stearate (A) and conversion to M+18 oleate (B). Uptake of M+16 palmitate and its conversion showed similar M+16 palmitate and M+16 palmitoleate (data not shown). M+0 stearate or palmitate represents mostly preexisting unlabeled fatty acid and a minor fraction of M+0 from the lack of recombination with M+2 acetate in new synthesis.

The changes found in the desaturation indices when SCD1 inhibitors or CLA were added may represent the inhibition of desaturase activity. However, these changes also reflect other alterations in the fatty acid metabolic network. For example, the significant decrease in the vaccenate/ stearate desaturation index with SCD1 inhibitors or CLA was likely due to an increase in the production of stearate as well as inhibition of the desaturation of palmitate (Fig. 4A, B). As another example, when stearate and palmitate desaturation were blocked, stearate accumulated from lack of desaturation and from increased production from chain elongation (Fig. 1). Therefore, the increase in stearate contributed in part to the decrease of the desaturation index. Furthermore, different desaturation indices determined from the experiments using labeled stearate versus labeled palmitate suggest the presence of further unidentified influences when using the desaturation index as an estimation of enzyme activity. Although the decreases in the

desaturation index may very well represent enzyme inhibition, such as in the groups when inhibitors were added, these indices do not offer a complete picture of the changes caused by altered desaturase activity.

Use of [U-^{13}C]stearate and [U-^{13}C]palmitate and GC-MS allowed the evaluation of SCD1 activity and following of the saturated fatty acids through connecting pathways (Fig. 1). The measurement of labeled precursors to their respective products, expressed as the enrichment ratio of monounsaturated to corresponding saturated fatty acid, gave additional perspective on the SCD1 systems (Table 1). The desaturation indices using enrichment ratios are a function of oleate synthesis from the labeled stearate pool and palmitoleate synthesis from the labeled palmitate pool. There were observed differences between the conventional desaturation indices (no isotope) and the desaturation indices using enrichment ratios. If SCD1 inhibition occurs in a different site, or if precursor contribution and turn-
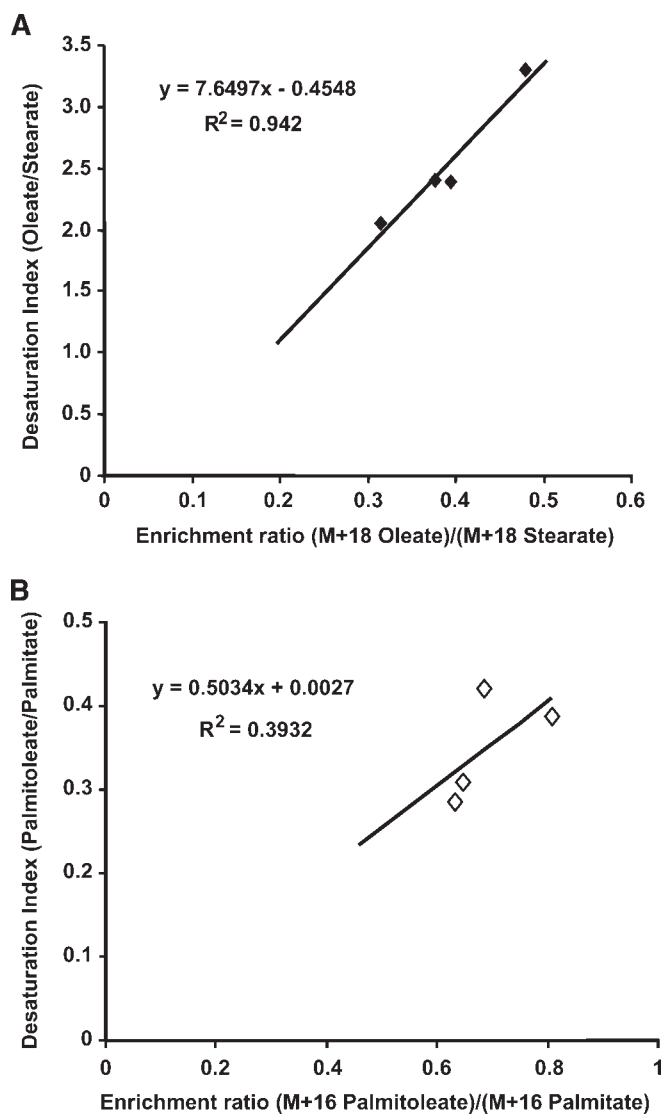
A

$y = 7.6497x - 0.4548$
$R^2 = 0.942$

Desaturation Index (Oleate/Stearate) (y-axis)
Enrichment ratio (M+18 Oleate)/(M+18 Stearate) (x-axis)

B

$y = 0.5034x + 0.0027$
$R^2 = 0.3932$

Desaturation Index (Palmitoleate/Palmitate) (y-axis)
Enrichment ratio (M+16 Palmitoleate)/(M+16 Palmitate) (x-axis)

Fig. 6. Correlation between the unlabeled oleate/stearate desaturation index and the (M+18 oleate)/(M+18 stearate) ratio (A) and between the unlabeled palmitoleate/palmitate desaturation index and the (M+16 palmitoleate)/(M+16 palmitate) ratio (B). The oleate pool in HepG2 cells is likely relatively large compared with the stearate pool (A). In this particular instance, the (M+18 oleate)/(M+18 stearate) ratio is linearly correlated with the oleate/stearate desaturation index.

over rates vary, the correlation between the conventional desaturation index and the enrichment ratio will be poor. However, under rare circumstances, such as a steady state, the conventional desaturation index may correlate to the desaturation index based on enrichment ratios, which is what we speculate may be the case shown in Fig. 6. The correlation is better for M+18 oleate/M+18 stearate, presumably because of slow turnover of oleate (Fig. 6). In this one instance, the conventional desaturation index reflects the overall consequence of the inhibition while the enrichment ratio provides pathway information. Therefore, using information from both methods provides a better estimate of SCD1 activity than either method alone. Use of stable isotopes may elaborate on the system further in future ex-

TABLE 2. Chain shortening and chain elongation

Group	Fraction of Palmitate from Chain Shortening of [U-^{13}C]Stearate Average ± SD	P	Fraction of Stearate from Chain Elongation of [U-^{13}C]Palmitate Average ± SD	P
	m_{16} palmitate/m_{18} stearate[a]		$m_{18} + m_{16}$ stearate/m_{16} palmitate[a]	
A (control)	0.0263 ± 0.0013		0.548 ± 0.070	
B	0.0423 ± 0.0008	<0.001	0.679 ± 0.054	0.031
C	0.0460 ± 0.0028	<0.001	0.705 ± 0.065	0.023
D	0.0539 ± 0.0006	<0.001	0.477 ± 0.147	0.248

Chain shortening is represented by the ratio m_{16} palmitate/m_{18} stearate. Chain elongation is represented by the ratio ($m_{18}+m_{16}$) stearate/m_{16} palmitate. m_{18} is made from M+16 palmitate and M+2 acetyl-CoA. The M+2 acetyl-CoA is derived from labeled palmitate oxidation and the exogenous [1,2-^{13}C]acetate.

[a] One minus the fraction of shortening or elongation equals the fraction contributed by unlabeled (preexisting) stearate or palmitate plus the fraction from de novo synthesis (m_2, m_4, etc.).

periments if appropriate time points for isotopomer measurements are included.

Of note, the desaturation indices based on the fatty acid enrichment ratios provide a measure of the desaturation of uniformly labeled fatty acid to the corresponding labeled monounsaturated product. Similar to the conventional desaturation index, this enrichment ratio is influenced by the rate of removal of monounsaturates, the input of monounsaturated products from other sources into the monounsaturated pool (e.g., de novo lipogenesis), and the desaturation of saturated fatty acids (i.e., SCD activity). For instance, after exposure to labeled saturated fatty acids, an increased rate of turnover or removal of MUFAs may increase the fraction of labeled saturated fatty acids independently of SCD1 activity, leading to an appearance of decreased SCD1 activity. However, there are circumstances in which changes in SCD1 activity can be reflected by the desaturation indices based on enrichment ratios. Since the source of labeled fatty acid precursor ([U-^{13}C]stearate or [U-^{13}C]palmitate) is not likely to affect

TABLE 3. Acetyl-CoA enrichment and de novo palmitate synthesis

Group	Acetyl-CoA Enrichment Average ± SD	P	Palmitate from de Novo Synthesis[a] Average ± SD	P
[U-^{13}C]stearate experiment				
A (control)	0.128 ± 0.0019		0.536 ± 0.0027	
B	0.128 ± 0.0015	0.484	0.538 ± 0.0047	0.298
C	0.135 ± 0.0011	0.003	0.513 ± 0.0100	0.009
D	0.130 ± 0.0008	0.052	0.520 ± 0.0184	0.104
[U-^{13}C]palmitate experiment				
A (control)	0.177 ± 0.005		0.465 ± 0.021	
B	0.185 ± 0.008	0.102	0.496 ± 0.003	0.033
C	0.198 ± 0.003	0.002	0.479 ± 0.026	0.262
D	0.174 ± 0.007	0.250	0.460 ± 0.037	0.412

[a] Of the fraction of palmitate that is not derived from chain shortening of fully labeled stearate (see Table 2), about 51–54% is from de novo synthesis of palmitate (m_2, m_4, etc.) and the remainder is from preexisting unlabeled palmitate. Of the fraction of palmitate that is not fully labeled, about 46–49% is from de novo synthesis of palmitate (m_2, m_4, etc.) and the remainder is from preexisting unlabeled palmitate.
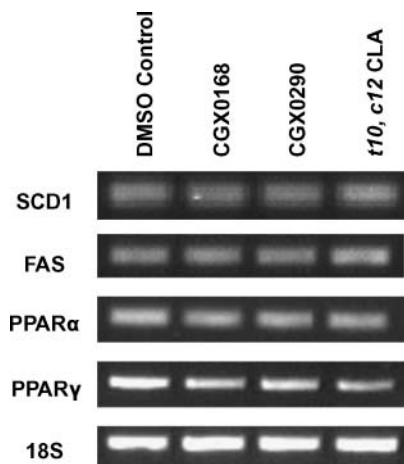
Fig. 7. Gene expression analysis of SCD1, FAS, peroxisome proliferator-activated receptor α (PPARα), and PPARγ by RT-PCR. 18S served as the internal loading control. There was no effect on gene expression from the addition of inhibitors CGX0168, CGX0290, or *trans*-10,*cis*-12 CLA.

either the turnover of the monounsaturated products or de novo synthesis, the explanations presented regarding compartmentalization are justifiable based on inferences from the enrichment ratios.

The dynamics of pathways other than desaturation can be measured using this tracer method. Higher acetyl-CoA enrichment was achieved in the [U-^{13}C]palmitate experiment in comparison with the [U-^{13}C]stearate experiment. Since the oxidation of [U-^{13}C]stearate or [U-^{13}C]palmitate also contributes to the [1,2-^{13}C]acetate pool, the higher enrichment observed in the [U-^{13}C]palmitate experiments suggests that HepG2 cells oxidize more of the added palmitate than the added stearate. The trend toward an increase in the calculated precursor enrichment suggests that β-oxidation of palmitate and stearate are potential competing reactions to the desaturation of saturated fatty acids.

Stable isotopes have been used previously as tracers to study compartmentalization of metabolic pathways (13). The analysis of enrichment ratios in this study suggested two ways in which the desaturase pathways are compartmentalized. First, desaturase activity appears to be compartmentalized according to the origin of the precursor (i.e., from chain elongation/shortening vs. exogenous). This is supported by the disparity in the enriched desaturation indices between the [U-^{13}C]stearate and [U-^{13}C]palmitate experiments, suggesting that desaturation of fatty acids from chain shortening or elongation occurs separately from desaturation of exogenous fatty acids. The desaturation index M+16 palmitoleate/M+16 palmitate was lower for palmitate derived from chain shortening than when the labeled palmitate was supplied exogenously. The enriched oleate/stearate desaturation index was higher when stearate was derived from chain elongation than when the stearate was supplied exogenously. If there was only one saturated fatty acid pool, then the palmitate-palmitoleate ratios should be similar for corresponding experimental groups and the oleate-stearate ratios should also be similar.

Since significant differences were observed between the measurements for each desaturation index, we propose the existence of several fatty acid compartments in which desaturation, chain shortening, and chain elongation take place.

The second way in which SCD1 activity may be compartmentalized is suggested by the fact that CLA did not inhibit palmitate desaturation, as reflected by the palmitoleate-palmitate ratio. If palmitate and stearate were in the same location being catalyzed by the same enzyme, one might expect that the rate of conversion to the monounsaturated fatty acids in the two pathways would be similar regardless of the source of the saturated fatty acid. *Trans*-10,*cis*-12 CLA was previously shown by Choi et al. (11) to decrease desaturation indices of palmitoleate and oleate, accompanied by a decrease in the direct measurement of SCD1 enzyme activity. However, in contrast to their results, our experiments showed that the SCD1 inhibitors and CLA decreased the conversion of stearate to oleate, but only the SCD1 inhibitors inhibited the palmitate-to-palmitoleate pathway. Such an observation may be explained by compartmentalization of SCD1 for these pathways, and CLA can access only one compartment but not the other. Although differential effects on turnover by SCD1 inhibitors or CLA may be a possibility, resulting in different desaturation indices for the palmitate versus stearate pathways, this cannot be validated within this project. An alternative explanation is that there may be yet another isoform of SCD1 that has not been identified and that both isoforms are susceptible to inhibition by CGX0290 and CGX0168, but only the stearate-to-oleate pathway is susceptible to inhibition by CLA. Notably, Miyazaki, Bruggink, and Ntambi (23) recently isolated a specific palmitate desaturase enzyme.

The recent discovery of this specific palmitate desaturase enzyme raises the possibility of a special metabolic role for palmitoleate as the precursor for vaccenate. Vaccenate is synthesized by the chain elongation of palmitoleate (Fig. 1), and its concentration is controlled by desaturation of palmitate as well as elongation of palmitoleate. It is conceivable that vaccenate and palmitoleate serve special metabolic functions different from that of oleate. There is evidence that vaccenate is converted by further desaturation to *cis*-9,*trans*-11 CLA (also known as rumenic acid) in humans (24).

No changes were found in gene expression by semi-quantitative RT-PCR with the addition of inhibitors or CLA. Therefore, in HepG2 tissue cells cultured with compound CGX0168, CGX0290, or *trans*-10,*cis*-12 CLA, changes in fatty acid composition by SCD1 inhibition are not associated with significant changes in gene expression. The mechanism of inhibition may work through metabolic fluxes at the posttranscriptional level. These findings are consistent with the observations of Choi et al. (11) and also with the findings of Hwang and Kang (25), who found that although there were decreased fat pad depots and triglyceride levels in male ICR mice fed CLA supplementation, gene expression of SCD1 was not changed in the livers. Since SCD1 inhibition by inhibitors was not complete, these inhibitors probably work as competitive inhibitors.

However, we cannot substantiate this within the scope of this project.

Evidence of resistance to diet-induced obesity and hypertriglyceridemia in animals with absence of SCD1 (8) and normalization of hepatic insulin resistance, gluconeogenesis, and glycogenolysis in animals after treatment with antisense oligonucleotide (9) have raised the hope that SCD1 can be targeted for the treatment of obesity and insulin resistance. Evidence in support of the role of SCD1 inhibition in the prevention and treatment of obesity is based on the diminished expression of SCD1 and a reduced desaturation index in the treated animals (8, 9, 26). Although desaturation is viewed as the rate-limiting step in triglyceride synthesis, inhibition of desaturation does not merely result in a decrease of monounsaturated fatty acids; it also leads to changes in chain elongation and chain shortening. The use of the conventional desaturation index offers limited information. Using stable isotopes and determining desaturation indices based on enrichment ratios provides an alternative method that presents additional pathway information. However, the use of both methods conveys a more complete picture than either method alone. The findings described show that inhibition of desaturation involves changes throughout the network of fatty acid metabolism. Therefore, an observed reduction of triglyceride synthesis may be the result of complex dynamics of fatty acid synthesis and turnover. Furthermore, compartmentalization of the palmitate and stearate desaturase systems suggests even further intricacies in the fatty acid metabolic network in HepG2 cells. How these different aspects of fatty acid metabolism work in an integrated fashion to reduce triglyceride synthesis and prevent insulin resistance remains to be investigated.∎

REFERENCES

1. Falvella, F. S., R. M. Pascale, M. Gariboldi, G. Manenti, M. R. De Miglio, M. M. Simile, T. A. Dragani, and F. Feo. 2002. Stearoyl-CoA desaturase 1 (*Scd1*) gene overexpression is associated with genetic predisposition to hepatocarcinogenesis in mice and rats. *Carcinogenesis.* **23:** 1933–1937.
2. Waresnjo, E., U. Riserus, and B. Vessby. 2005. Fatty acid composition of serum lipids predicts the development of the metabolic syndrome in men. *Diabetologia.* **48:** 1999–2005.
3. Wang, L., A. R. Folsom, Z. J. Zheng, J. S. Pankow, and J. H. Eckfeldt, for the ARIC Study Investigators. 2003. Plasma fatty acid composition and incidence of diabetes in middle-aged adults: the Atherosclerosis Risk in Communities (ARIC) Study. *Am. J. Clin. Nutr.* **78:** 91–98.
4. Wang, L., A. R. Folson, and J. H. Eckfeldt, for the ARIC Study Investigators. 2003. Plasma fatty acid composition and incidence of coronary heart disease in middle aged adults: the Atherosclerosis Risk in Communities (ARIC) Study. *Nutr. Metab. Cardiovasc. Dis.* **13:** 256–266.
5. Hulver, M. W., J. R. Berggren, M. J. Carper, M. Miyazaki, J. M. Ntambi, E. P. Hoffman, J. P. Thyfault, R. Stevens, G. L. Dohm, J. A. Houmand, et al. 2005. Elevated stearoyl-CoA desaturase-1 expression in skeletal muscle contributes to abnormal fatty acid partitioning in obese humans. *Cell Metab.* **2:** 251–261.
6. Zheng, Y., K. J. Eilertsen, L. Ge, L. Zhang, J. P. Sundberg, S. M. Prouty, K. S. Stenn, and S. Parimoo. 1999. Scd1 is expressed in sebaceous glands and is disrupted in the asebia mouse. *Nat. Genet.* **23:** 268–270.
7. Miyazaki, M., Y. C. Kim, M. P. Gray-Keller, A. D. Attie, and J. M. Ntambi. 2000. The biosynthesis of hepatic cholesterol esters and triglycerides is impaired in mice with a disruption of the gene for stearoyl-CoA desaturase 1. *J. Biol. Chem.* **275:** 30132–30138.
8. Ntambi, J. M., M. Miyazaki, J. P. Stoehr, H. Lan, C. M. Kendziorski, B. S. Yandell, Y. Song, P. Cohen, J. M. Friedman, and A. D. Attie. 2002. Loss of stearoyl-CoA desaturase-1 function protects mice against adiposity. *Proc. Natl. Acad. Sci. USA.* **99:** 11482–11486.
9. Gutierrez-Juarez, R., A. Pocai, C. Mulas, H. Ono, S. Bhanot, B. P. Monia, and L. Rossetti. 2006. Critical role of stearoyl-CoA desaturase-1 (SCD1) in the onset of diet-induced hepatic insulin resistance. *J. Clin. Invest.* **116:** 1686–1695.
10. Liu, G., J. K. Lynch, J. Freeman, B. Liu, Z. Xin, H. Zhao, M. D. Serby, P. R. Kym, T. S. Suhar, H. T. Smith, et al. 2007. Discovery of potent, selective, orally bioavailable stearoyl-CoA desaturase 1 inhibitors. *J. Med. Chem.* **50:** 3086–3100.
11. Choi, Y., Y. Park, M. W. Pariza, and J. M. Ntambi. 2001. Regulation of stearoyl-CoA desaturase activity by the *trans*-10, *cis*-12 isomer of conjugated linoleic acid in HepG2 cells. *Biochem. Biophys. Res. Commun.* **284:** 689–693.
12. Paul Lee, W. N., S. Lim, S. Bassilian, E. A. Bergner, and J. Edmond. 1998. Fatty acid cycling in human hepatoma cells and the effects of troglitazone. *J. Biol. Chem.* **273:** 20920–20934.
13. Wong, D. A., S. Bassilian, S. Lim, and W. N. Paul Lee. 2004. Coordination of peroxisomal beta-oxidation and fatty acid elongation in HepG2 cells. *J. Biol. Chem.* **279:** 302–309.
14. Pariza, M. W. 2004. Perspective on the safety and effectiveness of conjugated linoleic acid. *Am. J. Clin. Nutr.* **79 (Suppl.):** 1132–1136.
15. Talamo, B. R., and K. Bloch. 1969. A new assay for fatty acid desaturation. *Anal. Biochem.* **29:** 300–304.
16. Lowenstein, J. M., H. Brunengraber, and M. Wadke. 1975. Measurement of rates of lipogenesis with deuterated and tritiated water. *Methods Enzymol.* **35:** 279–287.
17. Rehan, V. K., S. Sugano, Y. Wang, J. Santos, S. Romero, C. Dasgupta, M. P. Keane, M. T. Stahlman, and J. S. Torday. 2006. Evidence for the presence of lipofibroblasts in human lung. *Exp. Lung Res.* **32:** 379–393.
18. Oberkofler, H., E. Schraml, F. Krempler, and W. Patsch. 2004. Restoration of sterol-regulatory-element-binding protein-1c gene expression in HepG2 cells by peroxisome-proliferator-activated receptor-γ co-activator-1α. *Biochem. J.* **381:** 357–363.
19. Cabrero, A., M. Cubero, G. Llaverias, M. Jove, A. Planavila, M. Alegret, R. Sanchez, J. C. Laguna, and M. V. Carrera. 2003. Differential effects of peroxisome proliferator-activated receptor activators on the mRNA levels of genes involved in lipid metabolism in primary human monocyte-derived macrophages. *Metabolism.* **52:** 652–657.
20. Lee, W. N., J. Edmond, L. O. Byerley, and E. A. Bergner. 1991. Mass isotopomer analysis: theoretical and practical considerations. *Biol. Mass Spectrom.* **20:** 451–458.
21. Lee, W. N., Z. K. Guo, and E. A. Bergner. 1992. Mass isotopomer pattern and precursor-product relationship. *Biol. Mass Spectrom.* **21:** 114–122.
22. Hellerstein, M. K. 1991. Appendix. Relationship between precursor enrichment and a ration of excess m_2/excess m_1 isotopomer frequencies in a selected polymer. *J. Biol. Chem.* **266:** 10920–10924.
23. Miyazaki, M., S. M. Bruggink, and J. M. Ntambi. 2006. Identification of mouse palmitoyl-coenzyme A Delta9-desaturase. *J. Lipid Res.* **47:** 700–704.
24. Turpeinen, A. M., M. Mutanen, A. Aro, I. Salminen, S. Basu, D. L. Palmquist, and J. M. Griinari. 2002. Bioconversion of vaccenic acid to conjugated linoleic acid in humans. *Am. J. Clin. Nutr.* **76:** 504–510.
25. Hwang, Y. H., and K. J. Kang. 2007. Conjugated linoleic acid reduces adipose depots without reduction of stearoyl coenzyme A desaturase gene expression. *Ann. Nutr. Metab.* **51:** 126–133.
26. Attie, A. D., R. M. Krauss, M. P. Gray-Keller, A. Brownlie, M. Miyazaki, J. J. Kastelein, A. J. Lusis, A. F. H. Stalenhoef, J. P. Stoehr, M. R. Hayden, et al. 2002. Relationship between stearoyl-CoA desaturase activity and plasma triglycerides in human and mouse hypertriglyceridemia. *J. Lipid Res.* **43:** 1899–1907.